

Research article – Optimisation of paediatrics computed radiography for full spine curvature measurements using a phantom: a pilot study

Cláudia Reis^a, Junior Ndlovu^b, Catarina Serrenho^a, Ifrah Akhtar^b, Seraphine de Haan^c, José Antonio Garcia^d, Daniel de Linde^e, Martine Thorskog^e, Loris Franco^d, Carla Lança^a, Peter Hogg^b

a) Lisbon School of Health Technology (ESTeSL), Polytechnic Institute of Lisbon, Portugal

b) School of Health Sciences, University of Salford, Manchester, United Kingdom

c) Department of Medical Imaging and Radiation Therapy, Hanze University of Applied Sciences, Groningen, The Netherlands

d) Haute École de Santé Vaud – Filière TRM, University of Applied Sciences and Arts of Western Switzerland, Lausanne, Switzerland

e) Department of Life Sciences and Health, Radiography, Oslo and Akerhus University College of Applied Science, Oslo, Norway



KEYWORDS

Optimisation
Spinal curvature Measurements
Effective dose
Image Quality
Paediatrics
Phantom
Computed radiography

ABSTRACT

Aim: Optimise a set of exposure factors, with the lowest effective dose, to delineate spinal curvature with the modified Cobb method in a full spine using computed radiography (CR) for a 5-year-old paediatric anthropomorphic phantom.

Methods: Images were acquired by varying a set of parameters: positions (antero-posterior (AP), postero-anterior (PA) and lateral), kilo-voltage peak (kVp) (66-90), source-to-image distance (SID) (150 to 200cm), broad focus and the use of a grid (grid in/out) to analyse the impact on E and image quality (IQ). IQ was analysed applying two approaches: objective [contrast-to-noise-ratio/(CNR)] and perceptual, using 5 observers. Monte-Carlo modelling was used for dose estimation. Cohen's Kappa coefficient was used to calculate inter-observer-variability. The angle was measured using Cobb's method on lateral projections under different imaging conditions.

Results: PA promoted the lowest effective dose (0.013 mSv) compared to AP (0.048 mSv) and lateral (0.025 mSv). The exposure parameters that allowed lower dose were 200cm SID, 90 kVp, broad focus and grid out for paediatrics using an Agfa CR system. Thirty-seven images were assessed for IQ and thirty-two were classified adequate. Cobb angle measurements varied between $16^{\circ} \pm 2.9$ and $19.9^{\circ} \pm 0.9$.

Conclusion: Cobb angle measurements can be performed using the lowest dose with a low contrast-to-noise ratio. The variation on measurements for this was $\pm 2.9^{\circ}$ and this is within the range of acceptable clinical error without impact on clinical diagnosis. Further work is recommended on improvement to the sample size and a more robust perceptual IQ assessment protocol for observers.

INTRODUCTION

There are several spinal deformities that can affect children, including scoliosis, kyphosis, lordosis, spondylosis and spondylolisthesis. Early diagnosis is paramount to improve life expectancy and quality. Amongst these deformities, scoliosis and kyphosis are identified as most common which can affect children during their early or late childhood¹⁻².

There are many methods of measuring spinal curvature including physical examination and other methods that require imaging (plain radiography, computed tomography (CT) and magnetic resonance imaging (MRI)). Imaging

is the most common and most accurate method to determine severity of curvature. Despite the enormous advances in cross-sectional imaging, plain radiography remains the mainstay for assessing spinal curvature³. It is used to confirm diagnosis, exclude underlying causes, assess curve and severity, monitor progression, assess skeletal maturation and determine patient suitability for surgery⁴.

Amongst the techniques that use imaging to measure spine curvature there are Cobb method, Centroid, TRALL & Harrison posterior tangent⁵. Cobb method is considered the gold standard for diagnosis and follow up. Nevertheless, it has been noted to have an error of up to $2^{\circ-7}$. However, a

more recent study by Hong et al⁸ showed better reliability with Cobb in comparison to other methods.

When performing Cobb angle measurements plain radiography involves radiation which involves an associated radiation risks. This is a particular concern in paediatrics because they are more sensitive to radiation due to faster cell division. Additionally, this may result to a high cumulative dose because of the series imaging related to the condition, increasing stochastic effects. Thus, it is paramount to keep doses As Low As Reasonably Practicable (ALARP)⁹. Therefore, it is vital to optimise IQ and dose; however, the lack of up-to-date paediatric guidelines makes it a challenge to choose the correct exposure parameters for digital systems. The most complete guideline found in the literature was the European guideline (EC)¹⁰ but it is out-dated as it is based on analogue systems. The most recent guidelines, such as the American College of Radiology (ACR)¹¹, are focussed on digital radiography, but it does not provide detail on exposure parameters for paediatrics. Furthermore, there are no published studies performed on this topic in radiography concerning paediatrics. For these reasons, this study aims to identify a set of exposure factors with the lowest effective dose to delineate spinal curvature using the modified Cobb method in a lateral full spine computed radiography (CR) for a 5-year-old paediatric phantom.

M E T H O D O L O G Y

This section describes the methodology followed in this study for data collection and analysis. It is organised in subdivisions corresponding to the four phases of the study:

- Phase 1: Image acquisition of spine radiographs achieved through manipulating the exposure parameters proposed by European Guidelines¹⁰.
- Phase 2: Effective dose estimation using PCXMC software (Monte Carlo simulation).
- Phase 3: Assessment of IQ using an objective measurement and a perceptual approach.
- Phase 4: Measurement of lateral spine curvature by using the modified Cobb method.

Phase 1 – Image acquisition

To perform image acquisition, a 5 year-old paediatric anthropomorphic phantom (Figure 1a and 1b), SIEMENS General X-ray unit (POLYDOROS IT 30/55/65/80 and OPTILIX 150/30/50C tube - inherent filtration 2.5mm Al @ 75 kVp) were used. The images were processed on an AGFA 35-X digitiser using a speed class of 400.

The image acquisition started with a pilot study performed in two stages. First stage was focused on alignment to guarantee that the phantom was placed in the central area of the automatic exposure control (AEC) system. On the second stage, the mAs and exposure time were collected using the AEC system for 70 acquisitions.

The pilot study provided exposure parameters to perform a total of 130 images on the phantom that were acquired in antero-posterior (AP), postero-anterior (PA) and lateral (LAT) positions using the technical exposure parameters recommended by EC guidelines¹⁰ (Table 1).

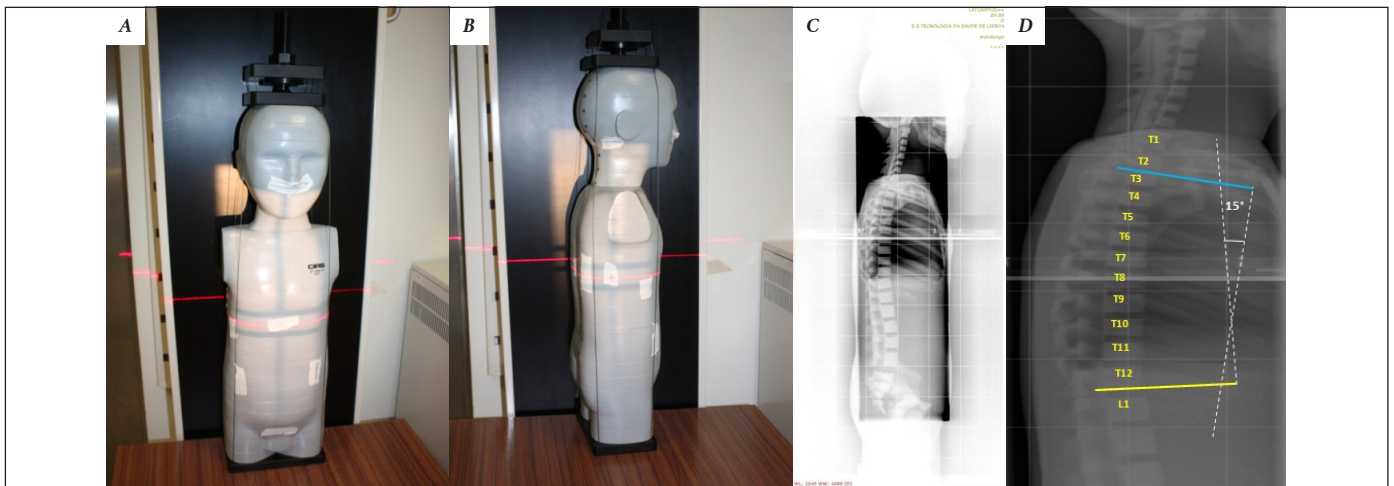


Figure 1: a) The anthropomorphic paediatric phantom in AP, and b) in lateral projection, c) the reference image of the phantom for perceptual image quality analysis, and d) modified Cobb angle measurement.

Table 1: Sets for image acquisition varying voltage (kVp), positioning, grid, source-to-image distance (SID) and focus

| Study Phases | Number of exposure performed | Number of images analysed | Manipulated parameters | | | | |
|---|------------------------------|---------------------------|------------------------|------------------------------------|---------------|-------------------|--------------|
| | | | Phantom Position | kVp range | Use Of Grid** | SID range [cm] | Focus |
| Phase 1 (Pilot): Alignment with AEC system | 3 | | 3 | AEC | In | 150 | AEC |
| Phase 1 (Pilot): collection of mAs and time (s) | 70 | | AP PA LAT | 66 71.5 77 81 85 90 | In & Out | 150 180 200 | Broad & Fine |
| Phase 1: Image acquisition | 130 | | AP PA LAT | 66 71.5 77 81 85 90 | In & Out | 150 180 200 | Broad & Fine |
| Phase 3: Perception of Image Quality | | 37* | LAT | 66 77 90 | In & Out | 150 180 200 | Broad & Fine |
| Phase 3: Cobb angle measurements | | 6* | LAT | 66 77 90 | Out | 150 180 200 | Broad |

Observation: AP: antero-posterior; PA: postero-anterior; LAT: lateral

* Images selected from the 130 acquisitions performed in phase 1

** Grid information: parallel; ratio=8 and absorbing Pb, strips

Phase 2 – Effective dose estimation

Effective dose (E) was calculated using PCXMC software¹. This software uses Monte Carlo simulation for calculating organ dose and E, for those who are examined with X-rays for medical use. By selecting the tissue weighting factors proposed by ICRP103 (mSv)¹², E was estimated using the exposure parameters (kVp, mAs), positioning, focal-skin distance, SID, age and beam size (collimation).

Phase 3 – Image analysis

The images were analysed using two approaches: objective, using the contrast-to-noise ratio (CNR) and perceptual, using observers.

Observers

Five observers performed perceptual image analysis: four radiographers with experience in paediatric radiology and familiar with Cobb angle and a radiography student.

These observers had their visual acuity assessed prior

to participating ((ETDRS chart – CSV 1000 and LogMAR Good-Lite chart), contrast sensitivity (CSV-1000E) and stereopsis (Randot)). Those who normally wore corrective lenses were asked to wear them during the vision testing. Binocular visual acuity for distance was -0.18 ± 0.04 LogMAR (20/13). All subjects had good visual acuity - LogMAR of -0.1 (20/16). All subjects had a normal near visual acuity (0.38 ± 0.04 M – 20/20) and stereoacuity (40.00 ± 0.00). The log average values of contrast sensitivity were similar to the population norms [13]: 3cpd (1.81 ± 0.13), 6cpd (2.20 ± 0.08), 12cpd (1.96 ± 0.07) and 18cpd (1.54 ± 0.02) spatial frequencies.

Image analysis using objective measurements

Thirty images (out of 130) were selected for CNR calculations. The inclusion criteria were the lateral projections in order to measure the Cobb angle (phase 4)¹⁴. The phantom does not present a curvature and for that reason the PA/AP projections were not analysed in this phase. The images acquired at 66, 77 and 90 kVp were selected (minimum, medium and maximum values of the range)¹⁰.

To calculate CNR, two regions of interest (ROI) were

marked on the images using a bespoke software (imageJ). ROI1 was applied mid-way of the vertebral body (maximum density) and ROI2 in the lung region with a homogenous density (minimum density) (Figure 2) and applied to the following formula (equation 1):

$$CNR = \frac{\text{Mean ROI2} - \text{Mean ROI1}}{\text{Standard deviation 1}}$$

The image with the highest CNR was selected as the reference image to perform the fourth phase of the study, which was acquired using fine focus (FF) with the grid inserted to ensure the AEC selected the optimum parameters visualised at 180cm SID.

Perceptual image analysis

To perform perceptual image analysis the previously selected images (30 out of 130) were transferred to a SIEMENS Syngo.via system with a monitor (SCD 1897-M) as used in clinical practice. Four images were selected to repeat the analysis including the reference image.

The images were analysed to determine if five relevant anatomical structures (see Table 2)^{10,14} were identifiable with the selected exposure parameters on a software tool ViewDEX (Viewer for Digital Evaluation of X-ray images). This software has been developed in Java and allows visual grading analysis (VGA) and image criteria scoring (ICS). The results from each observer were saved in a log file to be analysed using Excel and SPSS. It is a software that is DICOM compatible and the interface is easy to use¹⁵⁻¹⁶.

Table 2: Anatomical criteria used for perceptual image quality analysis applying a nominal scale (yes/no)

| Criteria | Appraiser combinations | |
|---|------------------------|----------|
| For the Cobb angle estimation, can you visualize the following? | Not adequate | Adequate |
| ... superior vertebral endplate | Yes/No | Yes/No |
| ... inferior vertebral endplate | Yes/No | Yes/No |
| ... inter-vertebral spaces | Yes/No | Yes/No |
| ... vertebral body | Yes/No | Yes/No |
| ... posterior vertebral body line | Yes/No | Yes/No |

Phase 4 – Cobb angle measurements

In this phase, seven digital images were selected (including lowest CNR, medium CNR, highest CNR and the reference) for drawing the Cobb angle stored on the AGFA IPD viewer system (ADC-QS). The lines to determine the Cobb angle were drawn along the superior and inferior vertebrae of the T3 and T12 respectively by each observer and ADC-QS automatically measured the angle (Figure 1d). Literature highlights the thoracic region as the most prominent for a spinal curvature in paediatrics¹⁷.

All images were anonymised to reduce bias. Before the task began, all observers were trained and the images used for the training were discarded from the study. A ten minute interval between this phase and the previous was allocated to minimise error¹⁸.

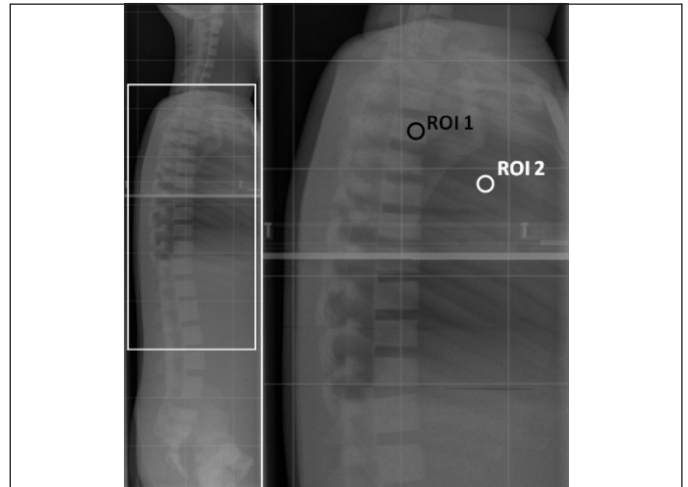


Figure 2: Lateral view showing Regions of Interest [ROI1 (vertebrae body) and ROI2 (lung)] to perform contrast-to-noise ratio (CNR) measurements.

All equipment is subject to regular quality control (QC). All equipment QC results fall with manufacturer specifications.

Statistical analysis

Data was analysed using Excel and SPSS to perform descriptive statistical analysis. Linear correlations (r^2) and Cohen's Kappa coefficients were also undertaken to observe the relationship between the variables and observers respectively. Five observers were used to determine the reliability for perceptual IQ. Kappa coefficients allow for the nominal scale used in the criteria to give statistical relevance to the study¹⁹. Three of the images were repeated three times to perform an inference sample and attain the standard deviation (StD) of the overall angle measurement. The StD was used to determine the level of accuracy for the angle measurements.

RESULTS

The results were sub-divided according to the dependent variables (E and IQ) and independent variables of position, kVp, the use of a grid and SID (see Table 1).

Effective dose

Under the conditions: 66 kVp, broad focus, no grid and 150cm SID, E was highest at images acquired in the AP position (0.048 mSv) when compared to PA (0.013 mSv). For lateral projection the E was lower than AP (0.025 mSv). When a grid was in use (AP - 0.097 mSv, PA - 0.041 mSv and lateral - 0.061 mSv), E was higher.

The use of a grid showed a moderate negative linear correlation at 150cm SID (-0.770) and a positive linear correlation at 200cm SID (0.7152). No correlation was identified for images acquired at 180cm SID (0.1141). In contrast, the image acquisition without a grid saw a stronger negative linear correlation at 180cm SID (-0.9265) whilst at 200cm SID (-0.7872), a moderate correlation was observed. The correlation weakens at 150cm SID (0.5127). E decreased at the higher kVp for 180cm and 200cm SID, however at 150cm SID, the data showed a moderate increase in E (Figure 3).

Image quality

The highest CNR was achieved at the lowest kVp of 66 consistently across all the categories (see Table 1). A strong negative linear correlation of -0.974 was reached for images acquired at 180cm and 150cm SID without a grid using 66, 77 and 90 kVp. Data also showed the highest SID of 200cm provided the highest CNR from the entire range of images acquired without a grid (Figure 4). Images acquired using a grid showed a similar trend with the highest CNR achieved at the lowest kVp at the SID of 200cm. No correlation was observed at 150cm SID (0.340) (Figure 5).

Concerning the perceptual IQ, thirty two images (out of 37) were classified as adequate because it is possible to visualise the anatomical criteria and five (out of 37) were classified as inadequate because one or more criteria not be identified by at least three observers.

The Kappa coefficient was used to calculate the reliability between each observer. The level of agreement for visualising the range of anatomical regions was good, however for anatomical regions not visualised, the level of agreement was very poor (-0.115 to 0.285) reducing the observer reliability using Kappa. Observer 1 compared to 2 demonstrated a moderate agreement (0.534).

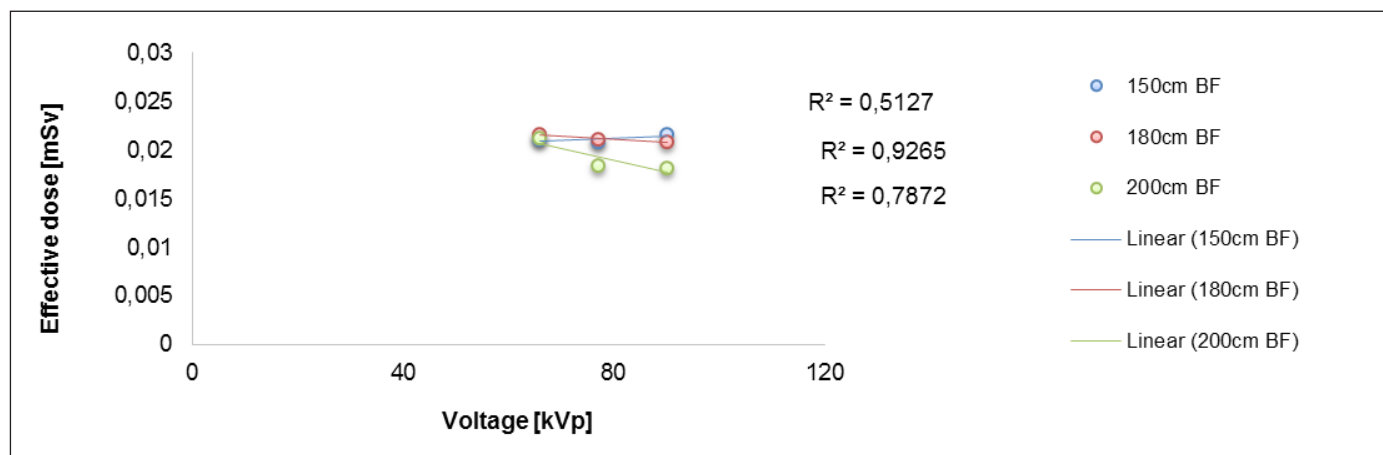


Figure 3: Comparison of effective dose for a range of kVp without grid for three sources to image distance (150, 180 and 200cm).

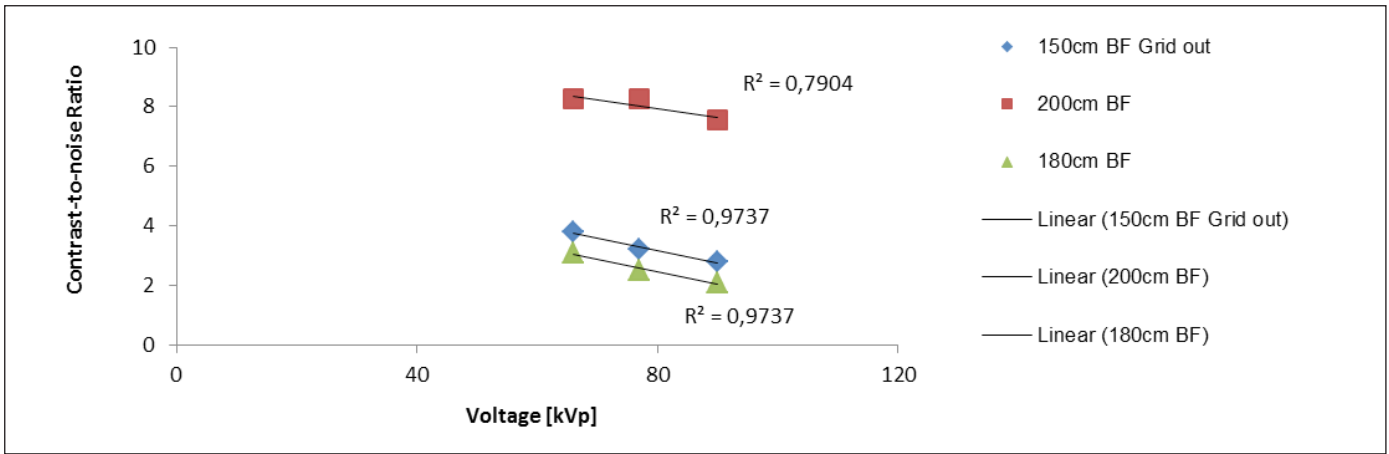


Figure 4: Comparison of contrast-to-noise ratio for images acquired using a range of kVp, broad focus (BF) and without grid for three sources to image distance (150, 180 and 200cm).

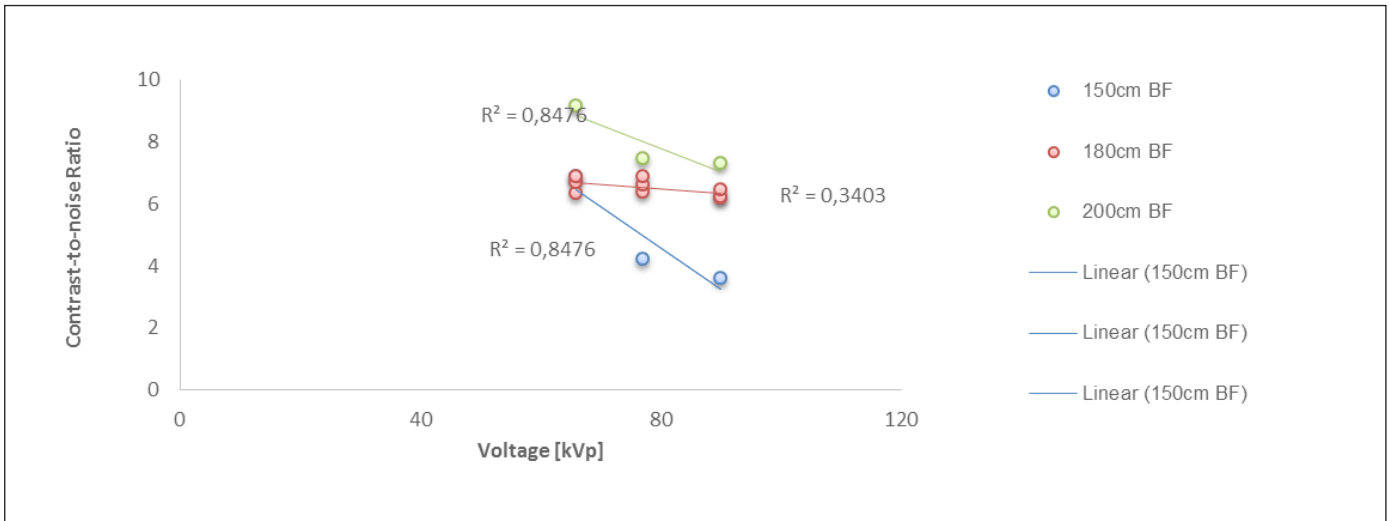


Figure 5: Comparison of contrast-to-noise ratio for images acquired using a range of kVp, broad focus (BF) and with grid for three sources to image distance (150, 180 and 200cm).

Table 3: Observers performance applying modified Cobb’s method to measure the spine curvature on lateral projections, the respective Standard-Deviation and image quality data concerning contrast-to-noise ratio and perceptual image quality

| Image | Mean Angle | Standard deviation | Contrast-to-noise ratio | Perceptual image quality |
|----------------|------------|--------------------|-------------------------|--------------------------|
| 85 (Reference) | 19.9 | 0.9 | 12.829 | Accepted |
| 91 | 16.4 | 2.3 | 9.139 | Accepted |
| 99 | 16.0 | 2.9 | 8.250 | Not accepted |
| 87 | 17.8 | 1.6 | 7.999 | Accepted |
| 12 | 19.0 | 2 | 3.611 | Accepted |
| 37 | 16.0 | 2.9 | 3.444 | Accepted |

Cobb angle measurement reliability

The statistical data for Cobb angle measurements are shown in (Table 3). The mean angle measurements showed

for the sampled images scored by the participants ranges from 16 to 19.9°. The mean StD varied between 0.9 to 2.9. The image with highest CNR (reference image) shows the lowest StD (0.9).

DISCUSSION

Many studies have examined the impact of exposure parameters on dose and IQ in spine radiography; however, there is a lack of studies on paediatrics combining several exposure parameters²⁰⁻²².

As noted within the results section, there are variations on E between different positioning, kVp range, grid and SID. The use of grid increased E as expected²³. This was most evident with the AP projection. AP projection had the highest E compared to PA and lateral and for that reason, sensitive organs are more exposed to radiation effects when this projection is used²⁴. Therefore, PA projection should be selected without grid for full spine examination on paediatrics to reduce E to optimise practice²⁰.

Literature suggests using larger SID as a strategy of reducing dose²⁵⁻²⁶. The results of this study are consistent with this as 200cm SID promoted lowest E. Concerning IQ, it was seen that the use of a larger SID increases CNR for the same kVp range because the AEC promotes uniformity of signal reaching the detector by increasing the mAs when kVp is reduced²³. For this reason a higher SID should always be selected for optimisation of the CR system used in this study.

The use of higher kVp is a well-known strategy to reduce dose on paediatrics, but at the same time can decrease CNR^{20,26}. On this study, it was shown that with higher kVp, the E is reduced for 180cm and 200cm SID, although this correlation was not as obvious for 150cm SID. This could be due to the small sample size used for this SID. The highest CNR was achieved at the lowest kVp of 66; this is consistent with Gardner¹⁸. This happens because with lower kVp there is less scatter radiation reaching the detector with increasing mAs due to AEC²³. Using a grid increases CNR as well as E²⁶. Despite this, the observers were able to detect all anatomical structures on an image with the lowest CNR obtained without a grid. This proves that dose can be reduced for this specific context. It also proves that physical (e.g., CNR) and perceptual measures of image quality do not always reflect how well the observer can perform in their diagnostic task.

Table 3 shows that the reference image has the lowest StD. This confirms a good agreement level between the observers. The highest StD was recorded at image with the lowest CNR (99) and medium CNR (37), suggesting disagreement between observers. The StD ranged from 0.9-2.9 and literature highlights that Cobb angle measurement with $\leq 2^\circ$, human error has no clinical impact^{6,27}. It was also noted that image 99 (which did not fulfil all five criteria), the observers

were still able to measure Cobb angle. This proves that Cobb angle can still be measured on images with low E considering this study.

The highest agreement obtained for perceptual IQ was performed by observers 1 and 2. Observer 1 has the longest experience in clinical practice (more than 15 years) and observer 2 have more than five years of paediatric experience with a good understanding of the AGFA system for the perceptual scoring. Observers 4 and 5 had the lowest agreement using the Kappa coefficient when compared against all observers. Observer 4 struggled to understand the task in the initial phase and took the longest time to adapt due to the lack of experience in using the AGFA system. After training, observer 4 assessed one specific region (the coccyx) for intervertebral disc space as opposed to the entire paediatric spine, skewing the data. However, a decision to include the observer's data was taken due to the vast experience in paediatric oncological radiography. Although the paediatric experience was an advantage, the clinical aim of the experiment was different for this observer. Despite the lack of agreement amongst all observers, there is no statistical and clinical method for determining a standard. Further work is recommended.

The agreement on visualising well defined structures is strongest across all observers. This could be related to the perceptual aspect of image quality where contrast impacts the visualisation of structures in imaging, consistent with literature²⁸⁻²⁹. The images varied in contrast detail, confirmed by the variation in the observers ability to not agree on images with less defined anatomical structures. Conversely, although all five observers had normal contrast sensitivity, the sensitivity for observers 1 and 2 was lowest for the "low spatial frequency" (images with low contrast). This suggests that regardless of image quality, the observers were able to accurately draw the Cobb angle within the acceptable clinical limits ($\leq 2^\circ$)^{6,27}, however, the range of experience in assessing paediatric images may be a limiting factor to the lack of agreement. The poor agreement of observer 5 can be explained by their use of tools as they were the only observer to use post processing tools through the use of the window level and the zoom function. These aspects of experience are identified as a limitation to the study and a proposal for more experienced observers and a robust protocol for perceptual IQ assessments are recommended.

Limitations are evident in this study. The sample size is limited on the basis of the high range of parameters (grid, spot size, tube voltage and current, SID and position) that resulted in an inclusion criteria with a reduced sample size.

CONCLUSION

The purpose of this study was to optimise exposure parameters for full spine paediatric radiography. The analysis showed that using higher SID, a dose reduction can be achieved and also an improvement on CNR. Using higher kVp promotes lower E but at the same time can decrease CNR. However, it was possible to verify that when IQ is considered inadequate by the observers the clinical goal can be achieved in this context as the Cobb angle measurements were performed with a lower error. This also confirms that perception of IQ is dependent on the characteristics (e.g. perception, experience and visual characteristics) of the

observer. The optimal exposure parameters for full spine lateral computed radiography applied on paediatrics considering this specific context are 200cm SID, 90 kVp, broad focus and grid out.

ACKNOWLEDGEMENTS

We would like to give acknowledgement to ERASMUS for sponsoring the research project, to the five observers that participated in this study and to Patricia Franco that help to collect the images for this project.

REFERENCES

- Bruce Jr R, Fletcher N. Pediatric spinal deformities [Internet]. Emory Health Care; 2014 [updated 2015; cited 2014 Aug 12]. Available from: <http://www.emoryhealthcare.org/pediatric-orthopedics/conditions/spinal-deformity.html>
- SingHealth. Orthopaedic problems in children: spine deformity (scoliosis, kyphosis) and back pain [Internet]. SingHealth Group; 2014 [cited 2014 Aug 12]. Available from: <http://www.singhealth.com.sg/PatientCare/ConditionsAndTreatments/Pages/Orthopaedic-Problems-in-Children-Back-Pain-and-Spine-Deformity-in-Children-and-Adolescents.aspx>
- Malfair D, Flemming AK, Dvorak MF, Munk PL, Vertinsky AT, Heran MK, et al. Radiographic evaluation of scoliosis: review. *AJR Am J Roentgenol.* 2010;194(s Suppl):S8-22.
- Rajiah P. Idiopathic scoliosis imaging [Internet]. Medscape; 2013 [cited 2014 Aug 12]. Available from: <http://emedicine.medscape.com/article/413157-overview>
- Harrison DE, Cailliet R, Harrison DD, Janik TJ, Holland B. Reliability of centroid, Cobb, and Harrison posterior tangent methods: which to choose for analysis of thoracic kyphosis. *Spine (Phila Pa 1976).* 2001;26(11):E227-34.
- Tanure MC, Pinheiro AP, Oliveira AS. Reliability assessment of Cobb angle measurements using manual and digital methods. *Spine J.* 2010;10(9):769-74.
- Chen YL, Chen WJ, Chiou WK. An alternative method for measuring scoliosis curvature. *Orthopedics.* 2007;30(10):828-31.
- Hong JY, Suh SW, Modi HN, Lee JM, Park SY. Centroid method: an alternative method of determining coronal curvature in scoliosis. A comparative study versus Cobb method in the degenerative spine. *Spine J.* 2013;13(4):421-7.
- Health and Safety Executive. ALARP "at a glance" [Internet]. HSE; 2014 [cited 2014 Aug 12]. Available from: <http://www.hse.gov.uk/risk/theory/alarplance.htm>
- Kohn M, Moores B, Schibilla H, Schneider K, Stender H, Stieve F, et al. European guidelines on quality criteria for diagnostic radiographic images in paediatrics. Luxembourg: Office for Official Publications of the European Communities; 1996.
- American College of Radiology. ACR – SPR – SSR Practice parameters for the performance of radiography for scoliosis in children [Internet]. Iowa: ACR; 2014 [cited 2014 Aug 12]. Available from: <http://www.acr.org/~media/ACR/Documents/PGTS/guidelines/Scoliosis.pdf>
- ICRP. The 2007 recommendations of the International Commission on Radiological Protection [Internet]. Ottawa: ICRP; 2007 [cited 2014 Aug 20]. Available from: <http://www.icrp.org/publication.asp?id=ICRP Publication 103>
- Pomerance GN, Evans DW. Test-retest reliability of the CSV-1000 contrast test and its relationship to glaucoma therapy. *Invest Ophthalmol Vis Sci.* 1994;35(9):3357-61.
- Al Qaroot B, Hogg P, Twiste M, Howard D. A systematic procedure to optimise dose and image quality for the measurement of inter-vertebral angles from lateral spinal projections using Cobb and superimposition methods. *J XRay Sci Technol.* 2014;22(5):613-25.

15. Håkansson M, Svensson S, Båth M, Månsson LG. ViewDEX: a java-based software for presentation and evaluation of medical images in observer performance studies. In Cleary KR, Miga MI, editors. *Medical imaging 2007: visualization and image-guided procedures* [Internet]. SPIE; 2007 [cited 2014 Aug 12]. p. 65091R. Available from: <http://proceedings.spiedigitallibrary.org/proceeding.aspx?articleid=1299200>
16. Börjesson S, Håkansson M, Båth M, Kheddache S, Svensson S, Tingberg A, et al. A software tool for increased efficiency in observer performance studies in radiology. *Radiat Prot Dosimetry*. 2005;114(1-3):45-52.
17. Cassidy CR, Calhoun JH. Kyphosis [Internet]. Medscape; 2013 [cited 2014 Aug 20]. Available from: <http://emedicine.medscape.com/article/1264959-overview>
18. Gardner A. Clinical assessment of scoliosis. *Orthop Trauma*. 2011;25(6):397-402.
19. Blackman NJ, Koval JJ. Interval estimation for Cohen's kappa as a measure of agreement. *Stat Med*. 2000;19(5):723-41.
20. Willis CE. Optimizing digital radiography of children. *Eur J Radiol*. 2009;72(2):266-73.
21. Schaetzing R. Management of pediatric radiation dose using Agfa computed radiography. *Pediatr Radiol*. 2004;34 Suppl 3:S207-14.
22. Hess R, Neitzel U. Optimizing image quality and dose for digital radiography of distal pediatric extremities using the contrast-to-noise ratio. *Rofo*. 2012.184(7):643-9.
23. Barnes GT. Contrast and scatter in X-ray imaging. *Radiographics*. 1991;11(2):307-23.
24. Young KJ. Should plain films of the lumbar spine be taken in the posterior-to-anterior or anterior-to-posterior position? A study using decision analysis. *J Manipulative Physiol Ther*. 2007;30(3):200-5.
25. Joyce M, McEntee M, Brennan PC, O'Leary D. Reducing dose for digital cranial radiography: the increased source to the image-receptor distance approach. *J Med Imaging Radiat Sci*. 2013;44(4):180-7.
26. Parry R, Glaze S, Benjamin A. The AAPM/RSNA physics tutorial for residents: typical patient radiation doses in diagnostic radiology. *Radiographics*. 1999;19(5):1289-302.
27. Tung CJ, Tsai HY, Shi MY, Huang TT, Yang CH, Chen IJ. A phantom study of image quality versus radiation dose for digital radiography. *Nucl Instrum Methods Phys Res A*. 2007;580(1):602-5.
28. Shah M. Electronic booking of hospital appointments Hippocrates of Cos and apoptosis For personal use. *The Lancet*. 2003;361(9365):1306.
29. Lança L, Franco L, Ahmed A, Harderwijk M, Marti C, Nasir S, et al. 10 kVp rule – An anthropomorphic pelvis phantom imaging study using a CR system: impact on image quality and effective dose using AEC and manual mode. *Radiography*. 2014;20(4):333-8.